
Early-Frame [¹⁸F]Florbetaben PET/MRI for Cerebral Blood Flow Quantification in Patients with Cognitive Impairment: Comparison to an [¹⁵O]Water Gold Standard

Ates Fettahoglu*^{1,2}, Moss Zhao*^{1,3}, Mehdi Khalighi¹, Hillary Vossler⁴, Maria Jovin¹, Guido Davidzon¹, Michael Zeineh¹, Fernando Boada¹, Elizabeth Mormino⁴, Victor W. Henderson⁴, Michael Moseley¹, Kevin T. Chen^{†5}, and Greg Zaharchuk^{†1}

¹Department of Radiology, Stanford University, Stanford, California; ²Radiology and Biomedical Imaging, Yale School of Medicine, New Haven, Connecticut; ³Stanford Cardiovascular Institute, Stanford University, Stanford, California; ⁴Department of Neurology and Neurological Sciences, Stanford University, Stanford, California; and ⁵Department of Biomedical Engineering, National Taiwan University, Taipei, Taiwan

J Nucl Med 2024; 65:306–312

DOI: 10.2967/jnumed.123.266273

Cerebral blood flow (CBF) may be estimated from early-frame PET imaging of lipophilic tracers, such as amyloid agents, enabling measurement of this important biomarker in participants with dementia and memory decline. Although previous methods could map relative CBF, quantitative measurement in absolute units (mL/100 g/min) remained challenging and has not been evaluated against the gold standard method of [¹⁵O]water PET. The purpose of this study was to develop and validate a minimally invasive quantitative CBF imaging method combining early [¹⁸F]florbetaben (eFBB) with phase-contrast MRI using simultaneous PET/MRI. **Methods:** Twenty participants (11 men and 9 women; 8 cognitively normal, 9 with mild cognitive impairment, and 3 with dementia; 10 β-amyloid negative and 10 β-amyloid positive; 69 ± 9 y old) underwent [¹⁵O]water PET, phase-contrast MRI, and eFBB imaging in a single session on a 3-T PET/MRI scanner. Quantitative CBF images were created from the first 2 min of brain activity after [¹⁸F]florbetaben injection combined with phase-contrast MRI measurement of total brain blood flow. These maps were compared with [¹⁵O]water CBF using concordance correlation (CC) and Bland–Altman statistics for gray matter, white matter, and individual regions derived from the automated anatomic labeling (AAL) atlas.

Results: The 2 methods showed similar results in gray matter ([¹⁵O]water, 55.2 ± 14.7 mL/100 g/min; eFBB, 55.9 ± 14.2 mL/100 g/min; difference, 0.7 ± 2.4 mL/100 g/min; *P* = 0.2) and white matter ([¹⁵O]water, 21.4 ± 5.6 mL/100 g/min; eFBB, 21.2 ± 5.3 mL/100 g/min; difference, −0.2 ± 1.0 mL/100 g/min; *P* = 0.4). The intrasubject CC for AAL-derived regions was high (0.91 ± 0.04). Intersubject CC in different AAL-derived regions was similarly high, ranging from 0.86 for midfrontal regions to 0.98 for temporal regions. There were no significant differences in performance between the methods in the amyloid-positive and amyloid-negative groups as well as participants with different cognitive statuses. **Conclusion:** We conclude that eFBB PET/MRI can provide robust CBF measurements, highlighting the capability of simultaneous PET/MRI to provide measurements of both CBF and amyloid burden in a single imaging session in participants with memory disorders.

Key Words: [¹⁸F]florbetaben PET; phase-contrast MRI; PET/MRI; cerebral blood flow

Cerebral blood flow (CBF) is an important biomarker in many neurologic disorders, including neurodegenerative and cerebrovascular diseases, and has been associated with changes in cognitive status (1–5). Subsequent work identified reduced CBF as a key component in early pathologic mechanisms and prognosis of Alzheimer disease (AD) and cognitive decline as well as in normal aging (6–9). Preclinical AD has been conceptualized as a synaptic disease, primarily driven by β-amyloid (Aβ) plaque and tau tangle deposition (10), yet cognitively normal individuals can present with elevated amyloid levels identical to those seen in AD pathology (11). Other biomarkers, including perfusion, may be relevant to neurodegeneration and cognitive decline (12). [¹⁵O]water PET is the gold standard for quantitative CBF measurements but is primarily limited to research facilities with an on-site cyclotron due to the tracer's extremely short half-life (~2 min).

Conceptually, early-frame PET imaging of lipophilic radiotracers with a high extraction fraction offers the potential to measure CBF using tracer kinetic methods, in which it is usually referred to as *K*₁. However, such quantification requires measurement of an arterial input function, which may require invasive arterial cannulation. This analysis method may be limited by uncertainties introduced by downstream radiotracer metabolites. Furthermore, the requirement for high temporal resolution leads to a lower signal-to-noise ratio in the individual frames. Despite these challenges, this dual use of a single PET agent is attractive because of the potential for simultaneously measuring both CBF and molecular binding information.

Previous studies using a range of tracers showed good correlation between early-frame PET imaging and CBF, but no studies have proposed a method to move from relative to absolute CBF measurements (13–16). One agent that has been proposed for such dual use is [¹⁸F]florbetaben, a tracer that in late time windows can image β-amyloid burden within the cerebral cortex, a necessary but nonsufficient condition for a diagnosis of AD (17). As such, [¹⁸F]florbetaben could be used to image 2 critical biomarkers in a single study evaluation, revealing a more complete picture of the

Received Jul. 2, 2023; revision accepted Oct. 24, 2023.

For correspondence or reprints, contact Kevin T. Chen (chenkt@ntu.edu.tw).

*Contributed equally to this work.

†Contributed equally to this work.

Published online Dec. 7, 2023.

COPYRIGHT © 2024 by the Society of Nuclear Medicine and Molecular Imaging.

vascular and molecular profiles of participants with cognitive decline. The aim of this study was to develop a method to quantify CBF by combining early [¹⁸F]florbetaben (eFBB) PET with phase-contrast MRI using simultaneous PET/MRI. The results were validated against gold standard [¹⁵O]water PET CBF measurements acquired in the same session.

MATERIALS AND METHODS

Study Design and Participants

This study was approved by the Stanford Institutional Review Board. All participants or their legally appointed representatives provided written informed consent before the imaging session. Participants were recruited through the Stanford Alzheimer Disease Research Center. This center reaches out to participants with memory issues and older, cognitively normal adults for the purposes of better understanding the pathophysiological changes related to dementia.

PET Image Acquisition and Reconstruction

All PET and MR images were acquired on a simultaneous time-of-flight-enabled 3-T PET/MRI scanner (Signa; GE Healthcare). Each participant received an intravenous injection of [¹⁵O]water (775 MBq) through the antecubital vein. Images were reconstructed using a time-of-flight ordered-subset expectation maximization algorithm with 3 iterations and 28 subsets, a nominal matrix size of 192 × 192, a field of view of 300 mm, and a slice thickness of 2.78 mm. At 20 min after the [¹⁵O]water PET imaging session, [¹⁸F]florbetaben (330 MBq) was injected in the same manner, and list-mode PET was acquired for a 20-min period. After the completion of the early-frame PET acquisition, participants were kept outside the scanner until the beginning of late-phase standard imaging in accordance with the [¹⁸F]florbetaben protocol. Static reconstructions were performed on list-mode data acquired between injection and 30, 60, 120, and 300 s to determine the optimal early-frame duration. The eFBB PET reconstruction was performed with the time-of-flight ordered-subset expectation maximization algorithm (3 iterations, 28 subsets) using the vendor's zero-echo-time method for attenuation correction and a 4-mm gaussian postreconstruction filter. Late-phase static [¹⁸F]florbetaben scans were also acquired between 90 and 110 min after injection to assess the amyloid burden of each participant.

MR Image Acquisition

Phase-contrast MRI was acquired for the quantitative measurement of blood flow velocity and vessel area in the internal carotid arteries and vertebral arteries simultaneously with the [¹⁵O]water PET session. A single-slice cardiac-gated fast low-angle gradient-echo sequence with the following parameters was used: TR/TE, 12/4.6 ms; flip angle, 20°; matrix size, 480 × 384; voxel size, 0.375 × 0.375 mm; slice thickness, 3 mm; number of averages, 2; and velocity encoding, 100 cm/s in the inferior to posterior direction. The placement of the imaging slices at the flexion of the vertebral artery at the second cervical vertebra, perpendicular to the internal carotid arteries and vertebral arteries, was confirmed by a noncontrast cervical MR angiogram. Fast spoiled gradient-echo T1-weighted anatomic MRI was simultaneously performed for estimating the whole brain volume, with the following parameters: TR/TE, 9.6/3.8 ms; flip angle, 13°; and voxel size, 0.94 × 0.94 × 1.0 mm.

CBF Quantification

Phase-contrast MRI flow data were analyzed with the Arterys platform (Arterys) using a region-growing algorithm to define the borders of the arterial lumen of the bilateral internal carotid and vertebral arteries. The blood flow in each vessel was determined by multiplying the flow velocity and area for each vessel and summing the measurements

to yield the total brain blood flow in units of mL/min. Total brain weight was derived from the volume measured by the T1-weighted anatomic image using the FSL Brain Extraction Toolbox (Analysis Group, FMRIB), assuming a brain tissue density of 1.1 g/mL, which included the ventricular and cerebrospinal fluid spaces. Mean whole-brain CBF was calculated from the total blood inflow divided by the total brain weight, yielding the traditional units of mL of blood/100 g/min (18). This value was used to scale both [¹⁵O]water PET and [¹⁸F]florbetaben early uptake to yield quantitative CBF maps (PC-eFBB).

Clinical Diagnosis and Amyloid Status

On the basis of the Uniform Dataset Clinician Diagnosis Form D1 (naccdata.org/data-collection/forms-documentation/uds-3), each participant's cognitive status and etiology were determined by Alzheimer Disease Research Center-affiliated neurologists. The cognitive status was established using the following classifications: normal cognition, mild cognitive impairment (MCI), and dementia. Because participants can have multiple cognitive statuses that may change throughout the years of enrollment at the Alzheimer Disease Research Center, the diagnosis date closest to the scan date was used for data analysis purposes. Amyloid status (Aβ positive [Aβ+] vs. Aβ negative [Aβ-]) was determined by the majority determination of 3 physicians trained to interpret [¹⁸F]florbetaben imaging (2 neuroradiologists with 17 and 13 y of experience and 1 nuclear medicine physician with 9 y of experience; all trained on interpreting amyloid PET imaging), on the basis of the 90- to 110-min [¹⁸F]florbetaben images.

Image Processing and Analysis

PC-eFBB and [¹⁵O]water PET images were preprocessed with FSL 6.0.5 (Analysis Group, FMRIB) using the following steps. The brain extraction tool was used to extract brain data from T1-weighted images, followed by FLIRT (FMRIB's Linear Image Registration Tool) rigid-body registration to the native T1-weighted images and finally nonlinear affine registration to the Montreal Neurologic Institute (MNI) 152 (MNI152) template space. Separation of gray matter and white matter volumes was performed by FAST (FMRIB's Automated Segmentation Tool) segmentation on T1-weighted images after the removal of cerebellum data. The automated anatomic labeling (AAL) atlas was overlaid on the MNI152 template-registered images using MRICroGL (version 12.3; <https://www.nitrc.org/projects/mricrogl>). Eight regions of interest (ROIs) corresponding to the cerebellar vermis, bilateral cerebellar hemispheres, midfrontal cortex, superior frontal cortex, inferior frontal cortex, occipital cortex, parietal cortex, and temporal cortex were extracted. Finally, voxel-by-voxel cross-correlation was performed for the purposes of determining the optimal early-frame length for [¹⁸F]florbetaben (between 30 s and 5 min). The optimal duration of the early frame for early [¹⁸F]florbetaben was selected on the basis of the highest correlation coefficient between eFBB and [¹⁵O]water CBF.

To obtain a voxelwise CBF difference map, the following steps were performed. [¹⁵O]water and PC-eFBB images of all of the participants were averaged in the template space. The averaged PC-eFBB images were then subtracted to obtain an error map. Two thresholds were applied to the error map (−5 to −25 and 5 to 25 mL/100 g/min) to avoid the near-zero noise floor, yielding under- and overestimation maps, respectively, which were overlaid on the T1-weighted structural image in the MNI152 template space. Data generated or analyzed during the study are available from the corresponding author by request, with a formal data sharing agreement and approval from the requesting researcher's local ethics committee.

Statistical Analyses

Statistical analyses were performed in Stata (version 17.0; <https://www.stata.com>). The Lin concordance correlation (CC) and Bland-Altman analysis with measurement of 95% limits of agreement were

used to assess CBF measurements in ROIs defined by the AAL atlas, and a paired 2-tailed *t* test was applied to determine significance using a *P* value of 0.05. Correlations within regions in separate individuals and between regions within individuals were both determined. For the latter, a summary statistic representing the median correlation and interquartile range was determined. The CC was calculated for white and gray matter measurements along with regression analysis by dividing the cohort according to cognition and amyloid burden. Regression analysis was used to determine whether there were significant differences in performance among patients with normal cognition, MCI, and dementia and between amyloid-positive and amyloid-negative participants.

RESULTS

Participant Demographics

Participants who were enrolled in the Stanford Alzheimer Disease Research Core program, which included patients with known or suspected neurodegenerative disease and healthy age-matched controls, and who had agreed to receive an amyloid PET/MRI study were offered the opportunity to participate in this additional [¹⁵O]water substudy. Of the 26 participants who enrolled in this substudy, 20 participants (9 women; mean age, 69y [SD = 9y]; 10 Aβ+ and 10 Aβ-) were included in the analysis. Six subjects did not complete the full imaging protocol, for the following reasons: 3 due to radiotracer delivery failure and 3 due to claustrophobia (Fig. 1). On the basis of the National Alzheimer Coordinating Center consensus criteria, 8 participants were cognitively normal, 9 had MCI, and 3 had dementia. The patients with cognitive impairment (MCI and dementia) had the following clinical diagnoses: AD (*n* = 5), corticobasilar degeneration (*n* = 2), dementia with Lewy bodies (*n* = 4), and cognitive impairment due to substance abuse (*n* = 1).

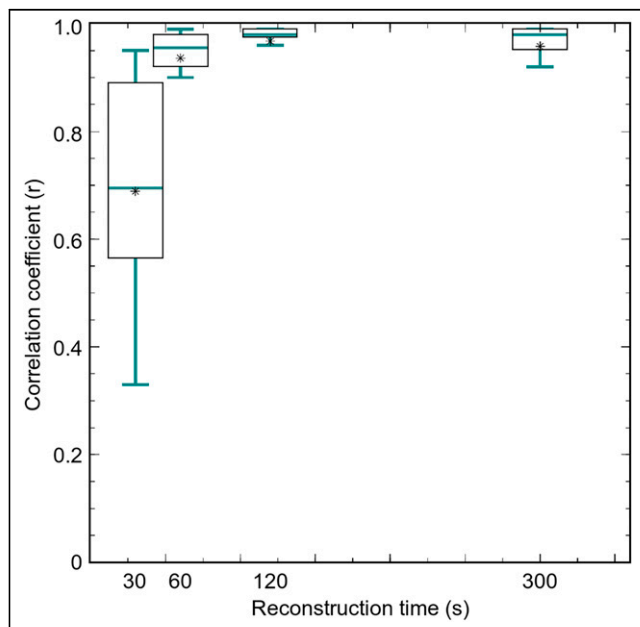


FIGURE 2. Whole-brain voxelwise cross-correlation (*r*) between [¹⁵O]water and eFBB CBF as function of eFBB reconstruction duration (30 s, 1 min, 2 min, and 5 min) after injection. Asterisk indicates mean, bar indicates median, box indicates first and third quartiles, error bars indicate ± 1 SD from mean.

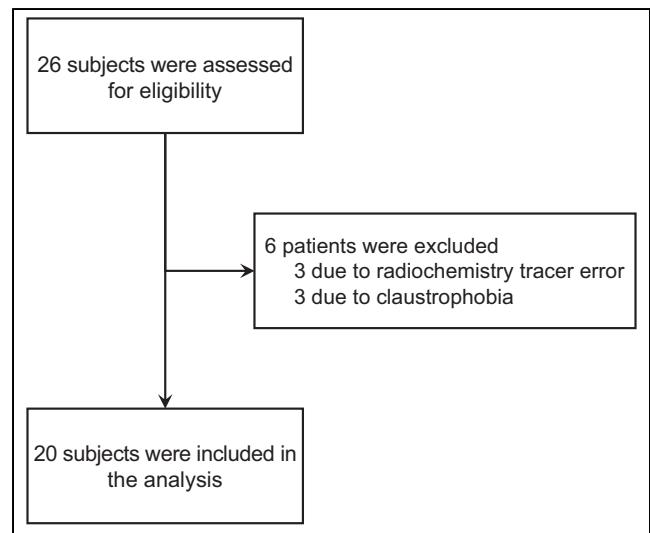


FIGURE 1. Flowchart for participant inclusion.

Determining Optimal Frame Length for eFBB

Voxelwise whole-brain correlation between [¹⁵O]water PET and eFBB CBF measurements are shown for different eFBB frame lengths (30 s, 1 min, 2 min, and 5 min) after injection in Figure 2; a 2-min frame length was chosen for subsequent analyses.

Comparison of [¹⁵O]Water and eFBB CBF

Mean whole-brain CBF measurements determined by [¹⁵O]water PET and eFBB were 40.1 ± 20.7 and 39.6 ± 19.9 mL/100 g/min, respectively. A comparison of CBF measurements using the 2 modalities in the 8 summarized AAL atlas ROIs is shown in Figure 3. CC coefficient values between [¹⁵O]water and eFBB for different AAL-based regions ranged from 0.86 to 0.98 (Table 1). There was no significant difference in the CC when the population was subdivided into amyloid-negative and amyloid-positive participants (CC, 0.90 vs. 0.87).

Mean whole-brain CBF measurements determined by the 2 methods were similar for gray matter (55.2 ± 14.7 mL/100 g/min vs. 55.9 ± 14.2 mL/100 g/min; *P* > 0.2) and white matter (21.4 ± 5.6 mL/100 g/min vs. 21.2 ± 5.1 mL/100 g/min; *P* > 0.4). Bland-Altman analysis demonstrated a bias of 0.7 ± 2.4 mL/100 g/min with 95% limits of agreement of 5.4 and -4.0 mL/100 g/min and -0.2 ± 1.0 mL/100 g/min with 95% limits of agreement of -2.2 and 1.8 mL/100 g/min for measurements in gray matter and white matter regions, respectively.

Regression analysis showed no statistical significance among different cognitive statuses with respect to measurements in gray matter (CC for cognitively normal, 0.98; CC for MCI, 0.98; CC for dementia, 0.98) and white matter (CC for cognitively normal, 0.99; CC for MCI, 0.98; CC for dementia, 0.99). Table 2 shows the correlation for the 115 AAL-generated regions for each participant in our study, demonstrating a median correlation of 0.92 (interquartile range, 0.87–0.93).

CBF images for representative participants with the 2 methods are shown in Figure 4, demonstrating similar visual appearances. An averaged CBF difference map measured on a voxel-by-voxel level is shown in Figure 5, demonstrating only small, scattered regions with absolute differences between the measurement methods on the order of 5–10 mL/100 g/min.

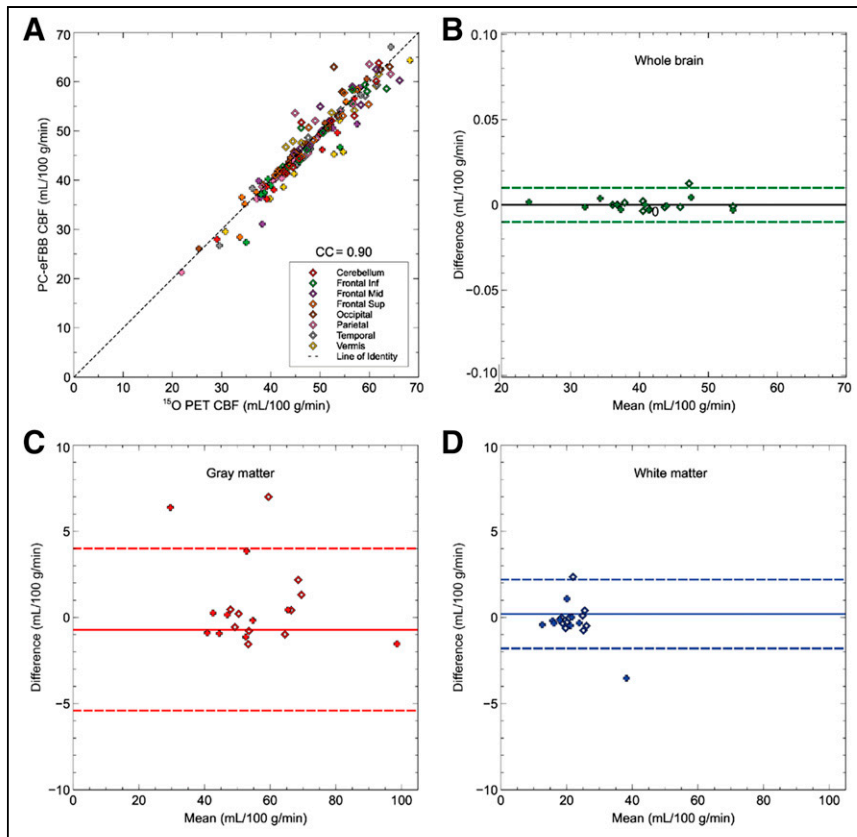


FIGURE 3. (A) Scatterplot of [^{15}O]water and eFBB CBF measurements for all regions in all subjects. (B–D) Bland–Altman analysis for whole brain (B), gray matter (C), and white matter (D) for all subjects. Bias is indicated by solid lines, and dashed lines represent 95% limits of agreement. Diamonds and plus symbols represent β -amyloid–negative and –positive cases, respectively. Inf = inferior; Sup = superior.

DISCUSSION

In the present study, we described and validated the use of eFBB imaging combined with MRI to determine quantitative CBF measurements. We first used voxel-by-voxel correlational analysis to determine an optimal early time frame for the eFBB measurement from our PET scanner. Although shorter frame lengths will be more highly CBF weighted, they will also have higher noise levels. To optimally trade off these 2 considerations, we chose a

2-min interval as opposed to other possible time frames (19,20). We then demonstrated equivalence in a cohort that included participants with normal cognition, MCI, and dementia, with equal representation of $\text{A}\beta^-$ and $\text{A}\beta^+$ participants. There was a strong correlation between [^{15}O]water and eFBB CBF measurements in whole brain, gray matter, white matter, and AAL-defined reference regions. Bland–Altman analysis revealed small biases of 0.7 and -0.2 mL/100 g/min between the measurements in gray matter and white matter, respectively. Given natural variability in blood flow in humans, this difference is negligible. Even variability as expressed by the 95% CI range was relatively small, from 5.4 to -4.0 mL/100 g/min. We did not see any difference in performance between $\text{A}\beta^-$ and $\text{A}\beta^+$ participants or in different groups based on cognitive status.

PC-eFBB is an absolute quantification method that uses phase-contrast MRI as a robust method to scale the relative perfusion map obtained from the initial eFBB PET images. Another method to calculate CBF from early-frame PET tracer data would be to use kinetic analysis with either arterial blood sampling or an image-derived input function (IDIF) (21). Arterial sampling is invasive, carries risk to the participant, and requires estimation of delay and dispersion, and prior studies suggested frequent failures due to blood clotting within arterial catheters (19,22).

The use of an IDIF obviates the need for invasive sampling but introduces additional variability due to the selection of the ROI and the relatively high noise of individual short-temporal-frame PET images required for capturing the early time points. Also, the need to set multiple parameters in the kinetic analysis adds additional variability. A scaling factor derived from phase-contrast MR images that measure whole-brain CBF is simple to use and

TABLE 1
Comparison of CBF Measurements Obtained with [^{15}O]Water and eFBB in Different AAL-Derived Regions

ROI	^{15}O water		eFBB		CC
	Mean	SD	Mean	SD	
Vermis	49.4	8.0	49.7	8.0	0.92
Cerebellum	48.6	8.4	48.5	8.8	0.90
Inferior frontal	47.3	8.3	49.2	8.8	0.86
Midfrontal	52.3	8.3	51.4	8.4	0.86
Superior frontal	47.4	8.1	48.3	8.3	0.90
Occipital	50.9	9.3	52.9	10.6	0.90
Parietal	46.9	9.4	47.8	9.8	0.92
Temporal	47.8	8.2	47.1	8.0	0.98

TABLE 2
CC of 115 AAL-Derived Regions in Individual Participants

Participant	Classification (NACC diagnosis)	Amyloid	CC*
1	MCI_LBD	Positive	0.95
2	Dementia_AD	Positive	0.95
3	Normal	Negative	0.93
4	MCI_LBD	Negative	0.95
5	Normal	Positive	0.87
6	Normal	Positive	0.76
7	MCI_CBD	Positive	0.70
8	Normal	Positive	0.93
9	MCI_IMPSUB	Negative	0.85
10	Normal	Positive	0.85
11	MCI_AD	Negative	0.90
12	Normal	Negative	0.93
13	MCI_LBD	Negative	0.91
14	MCI_CBD	Negative	0.88
15	Dementia_AD	Positive	0.93
16	Dementia_AD	Positive	0.87
17	MCI_LBD	Negative	0.93
18	MCI_AD	Positive	0.84
19	Normal	Negative	0.95
20	Normal	Negative	0.94

*Median = 0.92 (interquartile range, 0.87–0.93).

NACC = National Alzheimer Coordinating Center; LBD = dementia with Lewy bodies; CBD = corticobasilar degeneration; IMPSUB = cognitive impairment due to substance abuse.

has high reproducibility (23). The method highlights the value of simultaneous PET/MRI, with which simultaneous relative CBF images and the scaling factor for quantitation can be obtained to reduce physiologic variability. The range of whole-brain CBF values was as expected from an elderly population with mixed cognitive statuses. A recent review of CBF measurement comparisons between PET and arterial spin labeling reported that the correlation between the 2 methods was heavily influenced by the time interval between separate imaging sessions (24), emphasizing the day-to-day variability of CBF and the value of simultaneous data acquisition.

Previous research evaluated the suitability of eFBB for estimating CBF, but it yielded only relative measures (15–17,20,25). Kwon et al. investigated the optimal reference region for eFBB and reported a high correlation (r , 0.90) with ethyl cysteinate dimer SPECT using a cerebellar gray matter normalization approach (15). Daerr et al. compared images created from the first 5 or 10 min after [^{18}F]florbetaben injection with [^{18}F]FDG PET images, which demonstrated an appearance similar to CBF due to the relationship between blood flow and metabolism (20). They found correlations between 0.81 and 0.92 for a variety of ROIs through normalization to the global mean SUV ratio (20). Similar results were observed by Seiffert et al. in a comparison of 0- to 1-min amyloid images from 3 different ^{18}F tracers to [^{18}F]FDG images (25). Ottoy et al. evaluated 0- to 2-min early-frame [^{18}F]AV45 directly against several other tracers and metrics,

including [^{15}O]water, [^{18}F]FDG, and R1 (tracer delivery rate) estimated from [^{18}F]AV45 using tracer kinetics in a population similar to ours (16). They found correlations of 0.70–0.94 for different regions between early-frame [^{18}F]AV45 and [^{15}O]water PET but concluded that R1 better reflected disease severity than early-frame [^{18}F]AV45. It is important to note that all of these methods provided only correlations and, unlike our study, none was capable of deriving quantitative CBF from the amyloid images.

Heeman et al. reported variability in R1 measurements derived from kinetic modeling with [^{18}F]florbetapir and [^{18}F]flortaucipir in individuals with AD and cognitively normal individuals, where the latter tracer showed better repeatability (26). This was not the case for PC-eFBB, as we were able to demonstrate equivalence between A β [–] and A β ⁺ participants and among different cognitive groups. Bullich et al. demonstrated a noninvasive kinetic modeling approach with [^{18}F]florbetaben in a dual-time-window acquisition protocol similar to our experimental design (27). Alongside kinetic modeling, they applied an SUV ratio-based approach and concluded that the latter would be sufficient for most clinical applications, in which a compromise in accuracy is reasonable in favor of simplicity. Our approach showed high correlation as well as quantitative accuracy between the methods, likely due to our use of a simultaneous PET/MRI system. Although voxelwise differences in PC-eFBB and [^{15}O]water CBF were not reported at an individual level, AAL atlas ROIs were defined in 115 subregions, which sampled the CBF maps with

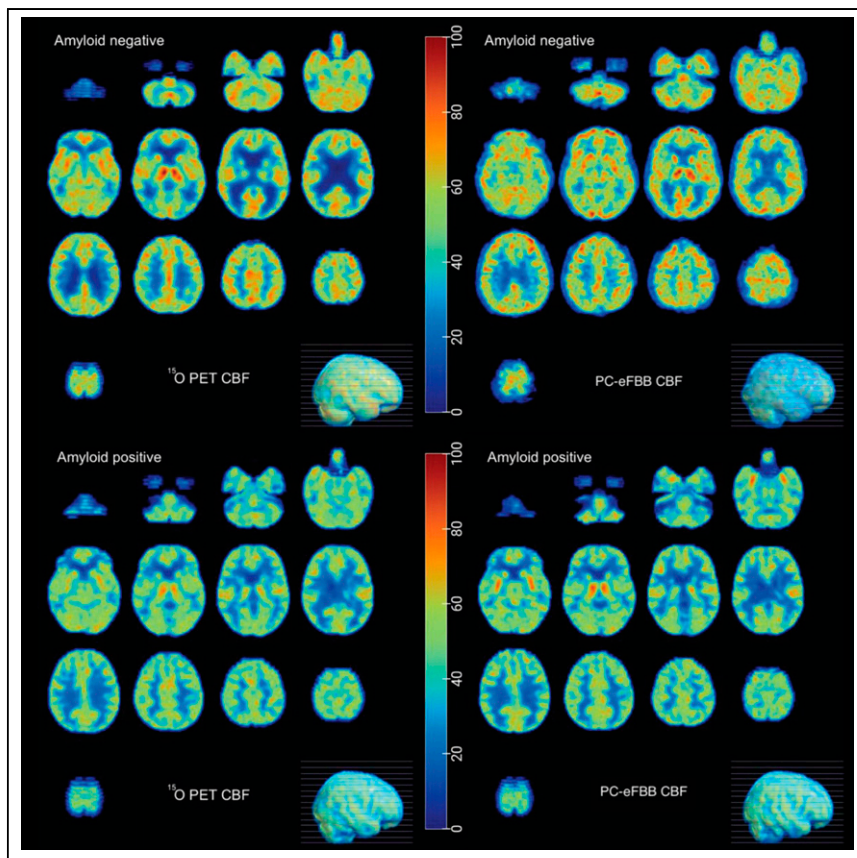


FIGURE 4. Representative [^{15}O]water PET and phase-contrast scaled eFBB CBF (PC-eFBB CBF) for representative β -amyloid-negative and -positive participants. Amyloid-positive participant had dementia that was ascribed to Alzheimer disease pathology. Amyloid-negative participant had normal cognition. Units of color bars measuring CBF are mL/100 g/min.

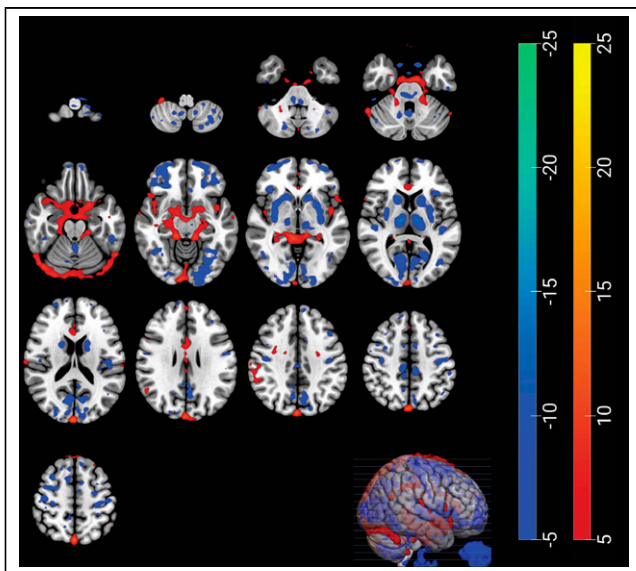


FIGURE 5. Voxelwise difference in CBF values measured using [^{15}O]water and eFBB averaged for all participants in units of mL/100 g/min. Red and blue represent regions where eFBB over- and underestimated CBF as measured by [^{15}O]water PET, respectively.

nearly voxelwise resolution and had the benefit of being more robust against complications such as small misalignment errors. As such, this approach will enable the measurement of both quantitative CBF and late-stage amyloid in the same participant with a single injection during a single imaging examination.

Our study has several limitations. eFBB could be validated in a larger and more diverse cohort, including more patients with dementia. Only a single PET/MRI scanner was used to acquire the imaging data and to derive the optimal early-frame reconstruction duration. This optimal time duration could vary with different PET scanners on the basis of their sensitivities. Next, we did not perform arterial sampling or obtain an IDIF to measure [^{15}O]water CBF. The latter was partially due to logistic limitations at our site surrounding arterial cannulation and our experience that these IDIF-based tracer kinetic measurements tend to be relatively unstable compared with phase-contrast MRI. Furthermore, our experimental protocol was not designed around the IDIF reconstruction method, and prior images (i.e., PET angiogram) were not rigorously validated during the acquisition.

The CBF quantification pipelines for [^{15}O]water and [^{18}F]florbetaben both depend on the Arterys-derived phase-contrast MRI measurements of the flow velocity and area in the bilateral internal carotid and vertebral arteries and are therefore limited by their accuracy (28). Other MRI-based CBF proxies, such as arterial spin labeling, could also be considered to normalize the relative PET CBF acquisitions. A final question might be why such a method is valuable at all, given that arterial spin labeling can measure CBF in studies that include MRI. Although arterial spin labeling can be used as a proxy for flow, its accuracy can be affected by susceptibility artifacts, unknown variations in labeling efficiency, changes in hematocrit that affect the T1 of the blood and, probably most importantly, prolonged arterial transit times (12). For these reasons, we believe that the eFBB approach could be more robust.

CONCLUSION

We have described and validated a hybrid PET/MRI method using eFBB and phase-contrast MRI to provide quantitative CBF measurements to complement late-phase amyloid assessment. As such, 2 important biomarkers may be measured in a single session in participants with memory concerns, enabling improved characterization of dementia pathophysiology with reduced cost and inconvenience to participants and their caregivers. Future studies could explore the use of other early-frame PET tracers and a similar methodology to provide additional quantitative CBF measurements in a wide range of diseases.

DISCLOSURE

This project was supported by National Institutes of Health grants P41-EB015891, R01-EB025220, K99-AG068310, R01-AG048076, and R21-AG058859; Stanford Alzheimer's Disease Research Center (P30-AG06615); Yushan Fellow Program by the Ministry of Education (Taiwan) NTU-112V1015-3; National Science and Technology Council (Taiwan) grant 110-2222-E-002-015-MY3; the Alzheimer's Association (AARFD-21-849349); GE Healthcare; Life Molecular Imaging; and American Heart Association grant 826254. Outside the submitted work, Greg Zaharchuk is a cofounder of and has an equity relationship with Subtle Medical Inc.; grant funding was supplied by GE Healthcare; and consulting fees were received from Biogen. No other potential conflict of interest relevant to this article was reported.

ACKNOWLEDGMENT

We thank Tie Liang for the statistical analysis.

KEY POINTS

QUESTION: Can a PET/MRI method for CBF measurement be developed using static early-frame [¹⁸F]florbetaben PET and phase-contrast MRI and validated with the reference standard [¹⁵O]water?

PERTINENT FINDINGS: When a CBF quantification method using eFBB and phase-contrast MRI was compared with the reference standard [¹⁵O]water, a high regional mean CBF CC (median CC, 0.92) was found in an elderly cohort including patients with a range of cognitive disorders. The eFBB CBF quantification method was accurate irrespective of amyloid pathology, and the optimal time frame for perfusion quantification was observed to be the first 2 min after injection.

IMPLICATIONS FOR PATIENT CARE: This approach is likely applicable to other lipophilic radiotracers, enabling CBF and molecular information to be measured in 1 setting in a dual-phase static PET/MRI acquisition.

REFERENCES

- de Heus RA, de Jong DL, Sanders ML, et al. Dynamic regulation of cerebral blood flow in participants with Alzheimer disease. *Hypertension*. 2018;72:139–150.
- Vestergaard MB, Lindberg U, Aachmann-Andersen NJ, et al. Comparison of global cerebral blood flow measured by phase-contrast mapping MRI with ¹⁵O-H₂O positron emission tomography. *J Magn Reson Imaging*. 2017;45:692–699.
- Kety SS, Schmidt CF. The effects of altered arterial tensions of carbon dioxide and oxygen on cerebral blood flow and cerebral oxygen consumption of normal young men. *J Clin Invest*. 1948;27:484–492.
- Appelman AP, van der Graaf Y, Vincken KL, et al. Total cerebral blood flow, white matter lesions and brain atrophy: the SMART-MR study. *J Cereb Blood Flow Metab*. 2008;28:633–639.
- Sabayan B, van der Grond J, Westendorp RG, et al. Total cerebral blood flow and mortality in old age: a 12-year follow-up study. *Neurology*. 2013;81:1922–1929.
- Korte N, Nortley R, Attwell D. Cerebral blood flow decrease as an early pathological mechanism in Alzheimer's disease. *Acta Neuropathol (Berl)*. 2020;140:793–810.
- Benedictus MR, Leeuwis AE, Binnewijzend MA, et al. Lower cerebral blood flow is associated with faster cognitive decline in Alzheimer's disease. *Eur Radiol*. 2017;27:1169–1175.
- Martin AJ, Friston KJ, Colebatch JG, Frackowiak RS. Decreases in regional cerebral blood flow with normal aging. *J Cereb Blood Flow Metab*. 1991;11:684–689.
- Albrecht D, Isenberg AL, Stradford J, et al. Associations between vascular function and tau PET are associated with global cognition and amyloid. *J Neurosci*. 2020;40:8573–8586.
- Braak H, Braak E. Neuropathological staging of Alzheimer-related changes. *Acta Neuropathol (Berl)*. 1991;82:239–259.
- Esparza TJ, Zhao H, Cirrito JR, et al. Amyloid-beta oligomerization in Alzheimer dementia versus high-pathology controls. *Ann Neurol*. 2013;73:104–119.
- Haller S, Zaharchuk G, Thomas D, et al. Arterial spin labeling perfusion of the brain: emerging clinical applications. *Radiology*. 2016;281:337–356.
- Blomquist G, Engler H, Nordberg A, et al. Unidirectional influx and net accumulation of PIB. *Open Neuroimag J*. 2008;2:114–125.
- Dishino DD, Welch M, Kilbourn M, Raichle M. Relationship between lipophilicity and brain extraction of C-11 labeled radiopharmaceuticals. *J Nucl Med*. 1983;24:1030–1038.
- Kwon SJ, Ha S, Yoo SW, et al. Comparison of early F-18 florbetaben PET/CT to Tc-99m ECD SPECT using voxel, regional, and network analysis. *Sci Rep*. 2021;11:16738.
- Ottoy J, Verhaeghe J, Niemantsverdriet E, et al. ¹⁸F-FDG PET, the early phases and the delivery rate of ¹⁸F-AV45 PET as proxies of cerebral blood flow in Alzheimer's disease: validation against ¹⁵O-H₂O PET. *Alzheimers Dement*. 2019;15:1172–1182.
- Yoon HJ, Kim BS, Jeong JH, et al. Dual-phase ¹⁸F-florbetaben PET provides cerebral perfusion proxy along with beta-amyloid burden in Alzheimer's disease. *Neuroimage Clin*. 2021;31:102773.
- Ishii Y, Thamm T, Guo J, et al. Simultaneous phase-contrast MRI and PET for noninvasive quantification of cerebral blood flow and reactivity in healthy participants and participants with cerebrovascular disease. *J Magn Reson Imaging*. 2020;51:183–194.
- Heijtel DF, Mutsaerts HJ, Bakker E, et al. Accuracy and precision of pseudo-continuous arterial spin labeling perfusion during baseline and hypercapnia: a head-to-head comparison with ¹⁵O H₂O positron emission tomography. *Neuroimage*. 2014;92:182–192.
- Daerr S, Brendel M, Zach C, et al. Evaluation of early-phase [¹⁸F]-florbetaben PET acquisition in clinical routine cases. *Neuroimage Clin*. 2016;14:77–86.
- Khalighi MM, Deller TW, Fan AP, et al. Image-derived input function estimation on a TOF-enabled PET/MR for cerebral blood flow mapping. *J Cereb Blood Flow Metab*. 2018;38:126–135.
- Ssali T, Anazodo UC, Thiessen JD, et al. A noninvasive method for quantifying cerebral blood flow by hybrid PET/MRI. *J Nucl Med*. 2018;59:1329–1334.
- Thunberg P, Karlsson M, Wigstrom L. Accuracy and reproducibility in phase-contrast imaging using SENSE. *Magn Reson Med*. 2003;50:1061–1068.
- Fan AP, Jahanian H, Holdsworth SJ, Zaharchuk G. Comparison of cerebral blood flow measurement with [¹⁵O]-water positron emission tomography and arterial spin labeling magnetic resonance imaging: a systematic review. *J Cereb Blood Flow Metab*. 2016;36:842–861.
- Seiffert AP, Gomez-Grande A, Villarejo-Galende A, et al. High correlation of static first-minute-frame (FMF) PET imaging after ¹⁸F-labeled amyloid tracer injection with [¹⁸F]FDG PET imaging. *Sensors (Basel)*. 2021;21:1–14.
- Heeman F, Visser D, Yaqub M, et al. Precision estimates of relative and absolute cerebral blood flow in Alzheimer's disease and cognitively normal individuals. *J Cereb Blood Flow Metab*. 2023;43:369–378.
- Bullich S, Barthel H, Koglin N, et al. Validation of noninvasive tracer kinetic analysis of ¹⁸F-florbetaben PET using a dual-time-window acquisition protocol. *J Nucl Med*. 2018;59:1104–1110.
- Wen B, Tian S, Cheng J, et al. Test-retest multisite reproducibility of neurovascular 4D flow MRI. *J Magn Reson Imaging*. 2019;49:1543–1552.